Quantitative Proteomic Analysis Shows Involvement of the p38 MAPK Pathway in Bovine Parainfluenza Virus type 3 Replication

Liyang Li
Heilongjiang Bayi Agricultural University https://orcid.org/0000-0002-4633-9419
Pengfei Li
The Fifth Affiliated Hospital of Harbin Medical University
Ao Chen
Heilongjiang Bayi Nongken University: Heilongjiang Bayi Agricultural University
Hanbing Li
Heilongjiang Bayi Agricultural University
Zhe Liu
Heilongjiang Bayi Agricultural University
Liyun Yu
Heilongjiang Bayi Agricultural University
Xilin Hou (houxilin@byau.edu.cn)

Research

Keywords: Bovine parainfluenza virus type 3 (BPIV3), Differentially expressed proteins, p38 MAPK signaling pathway, Quantitative proteomics

Posted Date: August 23rd, 2021

DOI: https://doi.org/10.21203/rs.3.rs-253558/v2

Quantitative proteomic analysis shows involvement of the p38 MAPK pathway in bovine parainfluenza virus type 3 replication

Liyang Li [a, b,1], Pengfei Li[c,1], Ao Chen[a], Hanbing Li[a], Zhe Liu[a], Liyun Yu [a*], Xilin Hou [b*]

a College of Life Science and Biotechnology, Heilongjiang Bayi Agricultural University, Daqing 163319, China

b College of Animal Science and Veterinary Medicine, Heilongjiang Bayi Agricultural University, Daqing 163319, China

c Department of Nephrology, The Fifth Affiliated Hospital of Harbin Medical University, Daqing 163319, China

1 These authors equally contributed to this work.

* Corresponding author. Tel.: +86 0459 6819291; fax: +86 0459 6819291.

E-mail address: houxilin@byau.edu.cn; yuliyun1227@126.com

Abstract

Background: Bovine parainfluenza virus type 3 (BPIV3) infection often causes respiratory tissue damage and immunosuppression and results in bovine respiratory disease complex. Bovine respiratory disease complex is one of the major diseases in dairy cattle and causes huge economical losses every year. The pathogenetic and immunoregulatory mechanisms involved in the process of BPIV3 infection, however, remain unknown. Proteomics is a powerful tool for high-throughput identification of proteins and has been widely used to understand how viruses interact with host cells. **Methods:** In the present study, we report a proteomic analysis to investigate the whole cellular protein alterations of MDBK cells infected with BPIV3. To investigate the infection process of BPIV3 and the immune response mechanism of MDBK cells, isobaric tags for relative and absolute quantitation analysis (iTRAQ) and Q-Exactive mass spectrometry-based proteomics were performed. The differentially expressed proteins (DEPs) involved in the BPIV3 invasion process in MDBK cells were identified, annotated, and quantitated. **Results:** A total of 116 proteins, which included 74 upregulated proteins and 42 downregulated proteins, were identified as DEPs between the BPIV3-infected and the mock-infected groups. These DEPs included corresponding proteins related to inflammatory response, immune response, and lipid metabolism. These results might provide some insights for understanding the pathogenesis of BPIV3. Fluorescent quantitative PCR and western blotting analysis showed results consistent with those of iTRAQ identification. Interestingly, the upregulated protein MKK3 was associated with the p38 MAPK signaling pathway. **Conclusions:** The results of proteomics analysis indicated BPIV3 infection could activate the p38 MAPK pathway to promote virus replication.

Keywords: Bovine parainfluenza virus type 3 (BPIV3); Differentially expressed proteins; p38 MAPK signaling pathway; Quantitative proteomics

Introduction

Bovine parainfluenza virus type 3 (BPIV3) is an enveloped, single-stranded negative-sense RNA virus that belongs to the family Paramyxoviridae, genus Respirovirus[1]. BPIV3 infection results in pneumonia and atypical interstitial pneumonia in cattle and leads to severe secondary bacterial infection and other related clinical symptoms. BPIV3 infection and other viral or bacterial infections often cause bovine respiratory disease complex (BRDC)[2]. The mortality of cattle due to BRDC is up to 35%, which causes huge economic losses in the cattle industry [3]. The genome of BPIV3 contains a single-stranded negative-sense RNA of approximately 15 kb in size and encodes six structural proteins and three nonstructural proteins [4, 5]. The structural proteins of BPIV3 include nucleoprotein (N), phosphoprotein (P), large protein (L), matrix protein (M), hemagglutinin-neuraminidase (HN), and the homotrimeric fusion (F), while the accessory nonstructural proteins include C, V, and D proteins. Multiple functions and activities of the structural and accessory proteins have been investigated. For example, the glycoprotein HN binds to the receptor protein on the host cell surface, followed by the fusion protein F to induce membrane fusion [6, 7]. The conserved, nonglycosolated matrix protein(M), is the most abundant viral protein in an infected cell. The nonstructural proteins including V protein and C protein are also encoded by the P gene. The V, C, and N proteins together regulate virus replication [5]. Although much progress has been made in understanding the proteins of BPIV3, the pathogenetic and immunoregulatory mechanisms involved in the process of BPIV3 infection remain largely unclear. To investigate the changes in the host physiological system during the process of viral invasion, isobaric tags for relative and absolute quantitation analysis (iTRAQ) mass spectrometry (MS)-based global proteomics profiling was performed.

The iTRAQ quantitative proteomics technique has been widely used to study interaction between virus and host based on high sensitivity and quantitation accuracy[8, 9]. An et al. used iTRAQ to determine the differentially expressed proteins (DEPs) of transmissible gastroenteritis virus (TGEV)-infected PK-15 cells. The authors identified 60 upregulated and 102 downregulated proteins in the TGEV infection process. Their analysis revealed that many upregulated proteins were associated with interferon signaling and that TGEV infection could activate the JAK-STAT1 signaling pathway [10]. Sun et al. used the iTRAQ quantitative proteomics technique to identify proteins associated with porcine epidemic diarrhea virus (PEDV) infection in order to provide a scientific basis for the pathogenesis of PEDV [11]. Presently, iTRAQ had become the main quantitative proteomics technology to understand the process of viral infection. In the present study, the DEPs in BPIV3-infected MDBK cells were identified and quantitatively analyzed by using an iTRAQ-based proteomics approach. MDBK cells have been selected for use in many studies [12, 13]. MDBK cells are commonly used not only for BPIV3 isolation, propagation and basic research, but also as hosts for many different bovine pathogens, including bovine respiratory syncytial virus (BRSV) and bovine herpesvirus type 1 [14, 15].

The expression levels of 116 proteins were found to be significantly altered after 24 h of

BPIV3 infection. These cellular DEPs were assigned to several biological processes according to bioinformatics analysis. The results of this study provide a global understanding of the host's immune response to BPIV3 infection.

Materials and methods

Virus infection of MDBK cells

MDBK cells were cultured in DMEM (Dulbecco's modified Eagle's medium) medium containing 10% fetal bovine serum (FBS) and 100g /ml penicillin and 100g /ml streptomycin. Cell culture conditions at 37 °C with 5% CO_2 in 24h. The BPIV3 DQ strain (GenBank accession no. HQ462571) was isolated and identified in the preventive veterinary laboratory of Heilongjiang Bayi Agricultural University. MDBK cells were transduction with BPIV3 at multiplicity of infection (MOI=1). Uninfected cells were used as mock-infected groups. Each experiment were carried out with three replicates. The cytopathic effect (CPE) was observed and the growth curve of BPIV3 was measured. $TCID_{50}$ were measured by the Reed-Muench method.

Protein isolation, digestion, and labeling with iTRAQ reagents

All the cells samples, included BPIV3-infected group and control group, were cleaned with cold PBS twice and centrifuged at 1000 g at 4 °C for 10 minutes to harvested cells. Then, the collected cells were lysed to extract proteins in the 300 μl SDT (1 mM PMSF, 2 mM EDTA and 10 mM DTT). Protein samples of dissolved were harvested with centrifugation at 1 4000 g for 40 min at 4 °C. The concentration of harvested protein supernatant was determined using BCA protein assay. Results showed that 100 μg protein was digested for 8 h at 37 °C using sequencing-grade modified trypsin. The protein samples were labeled by different iTRAQ tags on the basis of iTRAQ Reagent-8plex Multiplex Kit instruction (AB SCIEX). Three mock-infected samples were labeled by iTRAQ 113, iTRAQ 114, and iTRAQ 115, respectively; three BPIV3-infected samples were labeled by iTRAQ 116, iTRAQ 117 and iTRAQ 118, respectively. Then the labeled samples were mixed and dried by using vacuum concentrator.

LC-MS/MS Analysis

The labeled peptide samples were purified and separated by AKTA purification system. The operation methods and solution preparation were performed essentially as described previously [16]. The whole elution process was monitored at 214 nm and collected every minute. Thirty distillates were collected and neutralized in 10 pools and desalinated in a C18 cartridge. After each fraction was vacuum centrifuged, the sample was dissolved in 40 μL 0.1% trifluoroacetic acid and kept frozen at -80 °C for mass spectrometry analysis. Each sample was separated by capillary high-performance liquid chromatography (Thermo scientific EASY column (2cm, 100μm 5μm, C18). The chromatography conditions were as follow: Water with 0.1% formic acid (A) and Acetonitirile with 0.1% formic acid (B) were used as mobile phage. The flow rate was 300 nL per

minute and the mobile phage gradient program was used: 0-33 minute, from 0 % to 40%(B); 33-34 minute, B from 40 % to 100%(B); 34- 35minute maintained 100% and then back to 40%. Then, proteins were analyzed by using a Q-Exactive mass spectrometry (Thermo Finnigan) at positive ion mode (parameters: mass range: 300-1800m/*z*; Dynamic exclusion: 40.0 s, MS2 Activation Type: HCD, Normalized collision energy: 30eV).

Database search and bioinformatic analysis

MS/MS data were searched against the bovine subset database from the UniProt database (release March 22, 2016, containing 32 015 sequences) and proteins were identified by using Mascot 2.3.02. The peptide for quantification was automatically selected by Paragon™ algorithm to calculate the reporter peak area, error factor (EF) and p-value. The proteins expression levels of BPIV3-infected cells were calculated to compare with those of mock-infected cells. Proteins with fold changes >1.5 and p-values < 0.05 were considered as significantly different expressions. Auto bias-corrected were executed to decrease artificial error. These proteins were further classified using Gene Ontology (GO) and pathway enrichment analysis (http://www.geneontology.org).

RNA extraction and real-time PCR analysis

The mRNA level of differentially expressed proteins was analyzed by real-time PCR. Total RNA was extracted from cells of the BPIV3 infected group and the control group using TRIzol reagent (Takara) according to the manufacturer's protocol. The RNA concentration was measured using NanoDropnd-1000. After extraced, 1 μL total RNA was detected using electrophoresis. The cDNAs of these samples were obtained by reverse transcription. Relative quantitative real-time PCR was performed in a 25 μL system that containing 12.5 μL SYBR Premix Ex TaqTM II, 2 μL primers, 2 μL cDNA samples and 8.5μL water. The reaction condition was 95 °C for 10 min, then 40 cycles of 95 °C for 30 s, 57 °C for 30 s and 72 °C for 30 s, Then, the melting curves were obtained. The gene of GADPH was used as the internal reference gene. The data statistic was based on three independent experiments.

Table 1 The primers of genes (5′→3′)

Gene name	Acc. Number	Primer	Sequence	length
MHC Ⅱ	Q9TTM7	FwdRev	GAGCGAGTGTCATTTCTTCAAC	22
		Fwd	GCACGAACTCTTCTCCATTATG	22
GSTA1	A5PJE0	Rev	TCCAAGAGAGGGCAACAAAC	20
		Fwd	TCCACATAATAGAGCAATTCAACC	24
MKK3	A4IFH7	Rev	TGAAGCAGGTGGTAGAGGAG	20
		Fwd	CACGAAGGCAGCGATGTC	18
AP-2	P63009	Rev	GTGATTGCTGCTATGACTGTG	21
		Fwd	ATGTCTGGCTGACTCTTGG	19
MARCS	P12624	Rev	CTACAGTGCGGCTACAAATC	20
		Fwd	TGAAGAGGACAGAACAGAACC	21

Sep	P49907	Rev	GCTGGCTCTGGCTCTCTG	18
		Fwd	GGTGGAGGTTGCTTACAATAGG	22
FGF13	BC149415	Rev	GCTGAACGGAGGCAAGTC	18
		Fwd	TGATGGCAGATTAGAATAGTGAAC	24
TFPI	Q7YRQ8	Rev	GGCTGTGTTCTGCTAATGTC	20
		Fwd	AGTCTTGGCATCTTCTTGTTC	21
GADPH	AB098979	Rev	TTCAACGGCACAGTCAAGG	19
			CTCAGCACCAGCATCACC	18

Western-blot

MDBK cells were washed two times with PBS and disrupted with lysis buffer (50 mM Tris–HCl, pH 8.0, 150 mM NaCl and 1% Triton X-100, supplemented with 1 tablet of Complete-Mini Protease Inhibitor Cocktail per 50 ml buffer). Cell lysates were centrifugated at 12,000 × g for 10 min to harvest supernatants. Protein assays were performed on all supernatants using the Bradford method. For Western blot analysis of whole-cell lysates, samples, each containing 25–30 μg of protein equivalent, were dissociated in SDS-PAGE loading buffer and separated by 12% gradient SDS-PAGE. Proteins were then transferred to a nitrocellulose membrane. After sample separation by electrophoresis, proteins were transferred to an Immobilon-FL membrane (Millipore) via electroblotting. Primary anti-bodies and dilutions including MKK3 (rabbit, Cell Signal Technology5674, Danvers, MA), p38 phosphorylation (p-38) at 1:1000 (mouse, Cell Signal Technology9216, Danvers, MA), p-38 at 1:1000 (rabbit, Cell Signal Technology41666, Danvers, MA), β-actin at 1:10,000 (mouse, Sigma) and were incubated with membrane at 4 °C over-night. As a secondary antibody, anti rabbit immunoglobulin G (Santa Cruz Biotechnology Inc.) was applied (1:1000, rabbit or mouse) at room temperature for 1 h. After further washes, the immune complexes were revealed by enhanced chemluminescence using the ECL detection kit (Beijing Biosea Biotechnology Co., Ltd.).

Indirect immunofluorescent assay (IFA)

The operation methods were performed essentially as described previously [12]. MDBK cells were fixed with 4% paraformaldehyde for 10 min, permeabilized with 0.1% Trinton X-100 for 20 min, blocked with 1% BSA for 2 h, and washed with PBS three times. Cells were incubated with 200 μL rabbit polyclonal anti-BPIV3 serum (1:100) for 1 h, followed by incubation with 200 μL FITC-conjugated Goat anti-rabbit IgG (1:100) for 1 h at room temperature. The cells were washed extensively with PBS, and 90% glycerol was added to mount cells. Cells were examined and images were captured using fluorescence microscope.

Statistical analysis

Statistical analysis was performed in Microsoft Excel for two-tailed Student's t test or

one-way analysis of variance (ANOVA) and the p-values <0.05 were considered statistically significant.

Results

Detection of the activity of BPIV3 in MDBK cells

In proteomics analysis of virus-infected cells, the optimal sampling time is when the virus replicates quickly and the cells have no significant pathological effect (CPE). To determine the optimal sampling time point for proteomics analysis after BPIV3 infection, MDBK cells were cultured in a monolayer and inoculated with BPIV3. At different time points after inoculation, the cell-virus suspension was harvested at 6, 12, 18, 24, 36, 48, and 60 h, and $TCID_{50}$ was measured. The growth curve of BPIV3 was plotted according to the results of $TCID_{50}$. The results showed that BPIV3 proliferated rapidly from 24 to 36 h after infection, indicating active intracellular replication of the virus.

Because CPE is caused by intercellular fusion after BPIV3 invades the target cells, MDBK cells were inoculated with BPIV3 at the dose of 1 multiplicity of infection (MOI), and CPE was observed at different time points after infection. The results showed that lesions began to appear 12 h after BPIV3 infected the cells, and the lesions became more apparent with time (Fig. 1). The viral titer reached a plateau of approximately 5.7 log10 at 36 hpi and then gradually and continuously declined. Generally, the time point at which viral replication remains high but no signifificant host cell cytoskeleton or membrane rearrangement is observed is the optimal time for a proteomic analysis[12]. According to the post-infection cytopathic conditions combined with virus proliferation, cells infected at 24 h were used as the time point for proteomics analysis.

Protein profiling and iTRAQ quantification

The collected protein samples of BPIV3-infected and mock-infected MDBK cells were labeled with iTRAQ reagent in three biological repetitions. The quantitative information of the two experimental group ratios (ratio [infection/control]) was obtained by integrating the peptide segment information of three biological duplicates in the mock-infected group (control) and the BPIV3-infected group (infection).

The changes in the protein expression level between the two groups were analyzed based on statistical significance. A total of 2804 proteins were detected and quantified by LC-MS/MS. Among these proteins, 74 proteins were significantly upregulated and 42 proteins were markedly downregulated according to the change ratio of ≥ 1.5 for the proteins and significant differences at $P < 0.05$ (Fig. 2). The most significantly upregulated protein among the DEPs was vesicle-related membrane protein, which is related to autophagy. The most significantly downregulated protein was the integrin complement protein, which is a receptor protein of viral infection(Table.2).

Table2. The DEPs lists betweenBPIV3-infected group and mock group

NO.	Uniprot Accession no.	Protein name	GO annotation			P Value	V/C
			Biological Process	Cell Component	Molecular Function		
1	Q6PT99	Integrin beta	single organismal cell-cell;adhesionresponse to stimulus	plasma membrane region	integrin binding;molecular transducer activity; receptor activity	0.042	0.412
2	E1BEW4	Uncharacterized	regulation of cellular component organization	membrane	protein kinase activity; purine nucleotide binding	0.014	0.421
3	A7E337	OCRL protein	cellular component assembly;regulation of metabolic process	extracellular region part;cytoplasm	phosphatase activity; GTPase binding;	0.037	0.425
4	A5PJV9	DTYMK protein	metabolic process; biosynthetic process;	cytoplasm	nucleotide kinase activity;	0.034	0.497
5	Q9BE39	Myosin-7	biosynthetic process; metabolic process;	actin cytoskeleto; intracellular	binding	0.032	0.409
6	E1BF95	Uncharacterized protein	regulation of kinase activity;regulation of metabolic process	intracellular	purine nucleotide binding	0.048	0.420
7	A5PJX4	Mesoderm induction early response protein 2	regulation of primary metabolic process; regulation of cellular biosynthetic process	Nucleus; cellular_component	binding	0.037	0.466
8	E1BKT3	Uncharacterized protein	macromolecule localization; intracellular transport	plasma membrane region; membrane-	integrin binding	0.037	0.477
9	P49907	Selenoprotein P	signal transduction; G-protein coupled receptor signaling pathway	plasma membrane region; dendrite	signaling receptor activity;	0.042	0.480
10	Q0IIJ1	ERGIC and golgi 2	-	intracellular organelle; membrane-bounded organelle	-	0.044	0.483
11	G5E5P7	Uncharacterized protein	-	cytoskeleto; intracellular part	-	0.012	0.516

12	G3MZ53	N-acylglucosamine 2-epimerase	small molecule metabolic process	-	racemase and epimerase activity	0.006	0.524
13	F1N152	Serine protease HTRA1	regulation of metabolic process; signal transduction	Cytoplasm; extracellular matrix	serine hydrolase activity; insulin-like growth factor binding	0.002	0.527
14	Q3T0D7	GTP-binding protein SAR1a	macromolecule localization; cellular component assembly	endoplasmic reticulum; membrane-bounded vesicle	small molecule binding;	0.049	0.528
15	F1MDD5	Uncharacterized protein	developmental process;cell differentiation	extracellular organelle	receptor binding	0.007	0.529
16	F1MWI1	Clusterin	cell death;cellular process	-	-	0.002	0.533
17	O18973	Rab5 GDP/GTP ex-change factor	regulation of metabolic process; regulation of transport	Cytoplasm; recycling endosome	regulation of metabolic process	0.022	0.541
18	Q0VCC0	Calcyphosin	Metabolic process; regulation of cellular catabolic proces	cellular_component; intracellular part	cation binding	0.001	0.558
19	F1MS35	Uncharacterized protein	cellular component assembly;positive regulation of metabolic process	cytoplasmic vesicle; nucleus	cation binding;enzyme regulator activity	0.010	0.560
20	Q7YRQ8	Tissue factor pathway inhibitor 2	regulation of metabolic process; circulatory system development	membrane-bounded organelle;	endopeptidase regulator activity	0.000	0.563
21	Q32LB6	TATA box-binding protein-associated factor RNA polymerase I subunit D	regulation of metabolic process	membrane-bounded organelle	nucleic acid binding	0.031	0.566
22	E1BDC9	Uncharacterized protein	digestive tract development; cell differentiation	cytoplasm; endomembrane system	binding	0.032	0.570
23	F1N2K8	Uncharacterized protein	single-organism developmental process	cytoplasmic part	protein binding	0.007	0.578
24	F1MH50	Uncharacterized protein	regulation of cytoskeleton organizatio	cytoplasm	protein binding	0.001	0.579
25	G3N1L7	Uncharacterized protein		extracellular matrix	ion binding	0.004	0.582
26	Q9TTM7	MHC(BoLA) class II DR-beta chain	antigen processing and presentation	extracellular matrix;cytoplasmic part	binding	0.033	0.582

27	Q3ZC25	Transmembrane protein 106B	developmental process; cell morpho-genesis	Membrane; cytoplasm	-	0.002	0.582
28	E1BM92	Uncharacterized protein	single-multicellular organism process	plasma membrane region; cytoplasm	cytoskeletal protein binding	0.041	0.588
29	Q2KI45	Mitochondrial ribonuclease P protein 1	nucleic acid metabolic process	intracellular organelle; nucleoplasm	catalytic activity; transferase activity	0.033	0.594
30	M5FKH8	Periplakin	developmental process;	cytoskeleton ;intracellular part	binding	0.004	0.595
31	Q0P5F2	Proteasome assembly chaperone 1	cellular component assembly; organ development	cytoplasm; intracellular organelle	proteasome binding	0.035	0.597
32	E1B8X6	Uncharacterized protein	transport;	Intracellular; lysosome	-	0.009	0.607
33	A5PJE0	Glutathione S-transferase	metabolic process	intracellular part	transferase activity	0.016	0.607
34	A7MBJ4	Receptor-type tyrosine-protein phosphatase F	regulation of response to stimulus; cell development	membrane	anion bindin	0.025	0.608
35	Q5E9D6	Haloacid dehalogenase-like hydrolase domain-containing protein 3	small molecule metabolic process	-	hydrolase activity; phosphatase activity	0.015	0.612
36	F1MD78	Uncharacterized protein	-	intracellular organelle part; nuclear part	-	0.015	0.614
37	P34955	Alpha-1-antiprotein ase	regulation of metabolic process; negative regulation of catalytic activity	endoplasmic reticulum; intracellular organelle	glycoprotein binding; enzyme binding; enzyme inhibitor activity	0.044	0.617
38	A6QPZ3	NUP35 protein	transport	membrane	-	0.010	0.619
39	Q9MYM4	Lysosomal alpha-glucosidase	metabolic process	intracellular organelle; extracellular organelle	hydrolase activity	0.025	0.625
40	F1MJB0	Uncharacterized protein	-	-	-	0.013	0.626
41	E1BI31	Uncharacterized protein	positive regulation of immune system process	intracellular organelle; membrane	enzyme binding	0.040	0.629
42	Q3T0Y5	Proteasome subunit alpha type-2	cellular protein metabolic process;	extracellular vesicle;	endopeptidase activity	0.031	0.631

			multi-organism process	intracellular organelle			
43	F1MNT4	Uncharacterized protein	tissue development; regulation of cellular process	extracellular matrix	integrin binding	0.002	1.502
44	G3X839	Up-regulator of cell proliferation	apoptotic process	-	-	0.011	1.504
45	F1MPD4	Uncharacterized protein	-	-	-	0.000	1.508
46	G3MZ27	Uncharacterized protein	single-organism process	membrane part	trans-membrane signaling receptor activity	0.003	1.511
47	F1MHC3	CD44 antigen	cell adhesion	integral component of membrane	binding	0.000	1.512
48	G3X6B3	Uncharacterized protein	immune system process	membrane	nucleic acid binding	0.041	1.515
49	E1BBW0	Leucine-rich repeat flightless-interacting protein 2	-	cytoplasm; membrane	protein binding	0.009	1.530
50	A6QQN2	Tyrosine-protein phosphatase non-receptor type	apoptotic signaling pathway	endoplasmic reticulum	phosphatase activity	0.006	1.537
51	G5E6P8	Uncharacterized protein	lipid metabolic process	membrane	hydrolase activity	0.016	1.537
52	A5PKJ4	Mitogen-activated protein kinase 7	intracellular transport	cytoplasm	kinase binding	0.044	1.541
53	Q0VCX2	78 kDa glucose-regulated protein	regulation of cell migration	cytoplasmic vesicle	small molecule binding	0.000	1.542
54	A6QQ16	NSL1 protein	primary metabolic process	intracellular organelle	hydrolase activity	0.037	1.544
55	P17248	Tryptophan--tRNA ligase, cytoplasmic	metabolic process	intracellular organelle	binding	0.000	1.544
56	F1MWL1	Uncharacterized protein	cellular protein metabolic process	actin cytoskeleton	hydrolase activity	0.000	1.545
57	E1B7E1	Uncharacterized protein	regulation of developmental process	intracellular organelle	protein binding	0.027	1.546
58	Q58CU2	Band 4.1-like protein 5		cytoplasm; membrane	protein binding	0.011	1.555
59	Q9BE40	Myosin-1	metabolic process	intracellular organelle	binding	0.027	1.558
60	A6QL95	Dolichyl-diphospho oligosaccharide--protein glycosyltransferase subunit 1	cellular biosynthetic process	endoplasmic reticulum	catalytic activity	0.027	1.560
61	A8E641	DPYSL5 protein	developmental	cytoplasm	hydrolase activity	0.000	1.560

			process				
62	Q58D63	MOB kinase activator 3A		intracellular	cation binding	0.001	1.561
63	Q08E24	Store-operated calcium entry-associated regulatory factor	regulation of transport	intracellular organelle	-	0.041	1.565
64	Q08DW2	Phosphoribosyl pyrophosphate synthase-associated protein 1	compound metabolic process	-	transferase activity	0.005	1.578
65	F1MHH5	Uncharacterized protein	cell-cell adhesion	membran	signaling receptor activity	0.038	1.580
66	F1MMV5	Nuclear speckle-splicing regulatory protein 1	metabolic process	nucleus	binding	0.002	1.583
67	A4FV01	SF3B2 protein	-	intracellular	nucleic acid binding	0.027	1.585
68	A7E3V7	Guanine nucleotide-binding protein, beta-1 subunit	cellular response to organic substance	membrane part	hydrolase activity	0.004	1.604
69	A7YY73	Transcription factor MafF	organ development	intracellula	nucleic acid binding	0.001	1.610
70	G3MZZ3	Sorting and assembly machinery component 50 homolog	protein complex biogenesis	integral component of membrane	-	0.001	1.611
71	P01131	Low-density lipoprotein receptor	lipid metabolic process	plasma membrane raft	-	0.003	1.612
72	A4IFH7	MKK3 protein	inflammatory response	intracellular	protein kinase activity	0.002	1.619
73	A6QPP3	Fibroblast growth factor	single-organism developmental process	plasma membrane	kinase regulator activity	0.029	1.619
74	E1BIU0	Uncharacterized protein	cellular protein localization	membrane	binding	0.000	1.630
75	E1BJL9	Uncharacterized protein (Fragment)	regulation of immune system process	membrane	cytokine receptor binding	0.025	1.634
76	P63009	AP-2 complex subunit beta	intracellular protein transport	membrane	transporter activity	0.035	1.639
77	F1MPF7	Uncharacterized protein	developmental process	extracellular organelle	binding	0.001	1.653
78	P85521	Scavenger receptor cysteine-rich type 1 protein M130	inflammatory response	membrane	receptor activity	0.000	1.658
79	A4FUG6	ALG2 protein	protein metabolic process	cytoplasmic part	protein binding	0.000	1.660

80	F1MRP6	Collagen alpha-2(XI) chain		extracellular region	ion binding	0.001	1.668
81	E1BMF2	Uncharacterized protein	protein metabolic process	extracellular region	peptidase activity	0.002	1.677
82	F6R9F1	Uncharacterized protein	cellular response to stimulus	intracellular	binding	0.000	1.679
83	A8E4N3	Radial spoke head protein 3 homolog	-	-	-	0.031	1.680
84	Q32LE9	Cysteine and glycine-rich protein 2	developmental process	intracellular	ion binding	0.005	1.683
85	Q2TA45	Arf-GAP domain and FG repeat-containing protein 1	developmental process	membrane-bounded vesicle	enzyme regulator activity	0.035	1.686
86	A6QL93	TACC3 protein	response to stimulus	intracellular organelle	binding	0.000	1.687
87	P12624	Myristoylated alanine-rich C-kinase substrate		cytoplasm	protein binding	0.006	1.697
88	P33946	ER lumen protein-retaining receptor 1	regulation of transport	cytoplasmic part	peptide binding	0.005	1.705
89	F1MXI0	Kelch-like protein 9	metabolic process	intracellular part	transferase activity	0.033	1.713
90	A2VDK6	Wiskott-Aldrich syndrome protein fam-ily member 2	cell migration	extracellular region part	protein binding	0.006	1.717
91	G3N121	Cytosolic carboxypeptidase 3	protein metabolic process	cytoplasm	binding	0.034	1.717
92	F1MQ43	Uncharacterized protein	regulation of metabolic process	membrane	enzyme binding	0.000	1.737
93	Q7SIB2	Collagen alpha-1(IV) chain	single-organism process	extracellular region|	protein binding	0.002	1.763
94	E1BG99	Uncharacterized protein	regulation of metabolic process	-	-	0.000	1.852
95	E1B9F3	Uncharacterized protein	cellular developmental process	cytoplasm	protein binding	0.000	1.863
96	E1B7H4	Uncharacterized protein	response to stress	cytoplasm	protein kinase activity	0.002	1.885
97	F1MTZ0	Protein phosphatase inhibitor 2	regulation of signal transduction		enzyme regulator activity	0.000	1.891
98	F1MCR5	Fibronectin type 3 and ankyrin repeat domains protein 1	-	intracellular	-	0.000	1.901
99	Q08DQ1	Calcium/calmodulin -dependent protein kinase I	biosynthetic process	intracellular	nucleoside binding	0.001	1.927

100	A6QLU8	Nucleoredoxin	regulation of protein metabolic process	cytoplasm	antioxidant activity	0.004	1.949
101	F1MX40	Uncharacterized protein	metabolic process	nucleoside binding	nucleotide binding	0.000	1.959
102	Q9TRL9	CA(2+)-dependent carbohydrate-bindin g protein	regulation of developmental process	nucleus	binding	0.004	1.962
103	F1MJZ0	Uncharacterized protein	regulation of system process	membrane	signaling receptor activity	0.001	1.970
104	Q3T0C8	PDZ and LIM domain protein 2		cell junction	cation binding	0.002	1.979
105	E1B7M1	Uncharacterized protein	cellular developmental process	-	exchange factor activity	0.022	1.998
106	F1MQI1	Uncharacterized protein	cellular protein localization	intracellular organelle	receptor binding	0.021	2.085
107	F1MWF0	Uncharacterized protein	regulation of protein metabolic process	cytoplasmic vesicle	phospholipid binding	0.007	2.243
108	Q1LZB2	NCK adaptor protein 1	regulation of signaling	cell-cell junction	protein kinase inhibitor activity	0.001	2.252
109	G3MWY9	Sjoegren syndrome nuclear autoantigen 1 homolog	regulation of cellular process	cytoplasm	protein binding	0.000	2.254
110	E1BGM1	Uncharacterized protein	-	-	ion binding	0.001	2.294
111	E1BM72	Pescadillo homolog	primary metabolic process	Nucleus; membrane	nucleic acid bindin	0.028	2.434
112	A7YW40	Transcription elongation factor SPT5	metabolic process	Nucleus; intracellular	binding	0.000	2.604
113	F1MHA1	Uncharacterized protein	biological regulation	intracellular part	transferase activity	0.000	3.021
114	F1MSV7	Uncharacterized protein	regulation of secretion	intracellular	metal ion binding	0.008	3.075
115	G3X752	Vesicle-associated membrane protein 3	regulation of secretion	cytoplasm	binding	0.000	3.850
116	F1MJN7	Uncharacterized protein	-	-	binding	0.000	3.923

GO annotations of the DEPs

The results of the GO enrichment analysis of the biological process showed that the DEPs were significantly enriched in five processes. These processes included single organism process, response to a stimulus, metabolic process, cell process, and biological regulation. The proteins involved in the biological regulation process were found most, followed by those involved in the stimulation response process. In this study, the proteins involved in the stimulation response process mainly included tyrosine phosphatase, signal transduction protein 1 , Rab5 GDP/GTP

conversion factor 1 , interleukin-13 (IL-13), mitogen-activated protein kinase 7 (MAPK7), FOX transcription inhibitory factor 3(Foxp3) , calcium phosphate, protein tyrosine phosphatase protein receptor , MAP3K10, human telomerase reverse transcriptase , and SSNA1. IL-13 is the most important inflammatory factor that causes airway inflammation. It plays a key role in the occurrence of chronic airway inflammatory disease, which induces high secretion of mucus. Foxp3 is a member of the Fox transcription factor family that plays an important role in maintaining the immune function of the body[17]. The DEPs in BPIV3-infected MDBK cells may cause the initial cellular stress response. The precise role of these DEPs in the BPIV3 infection process need to be further investigated.

Kyoto Encyclopedia of Genes and Genomes (KEGG) pathway analysis of the DEPs

The KEGG pathway database is a collection map based on the molecular interaction pathways and cellular response networks. The DEPs were identified and mapped to six KEGG pathways, including metabolism, cellular processes, organismal systems, environmental information process, genetic information process, and disease pathways. The organismal systems and disease pathways were enrichment pathways, represented by 37 and 43 pathway groups, respectively.

In the metabolic pathways, the DEPs participated in 13 pathways related to the metabolism of glucose, lipid, amino acid, and nucleotides (Fig 4-A). These pathways affect the metabolism of three major nutrients in cells. The cellular processes involved ten pathways (Fig.4-B), including the Focal adhesion pathway and the Phagosome pathway, both of which are involved in the viral infection process; the integrin protein is the key protein in these two pathways. The lysosome pathway, phagosome pathway, and autophagy are involved in the autophagy process of virus infection. The annotated proteins in the category of genetic information processing play a role in the synthesis, transport, proteolysis, and spliceosome of cells (Fig.4-D). The annotated proteins in the organismal systems category were related to antigen processing and presentation, NOD-like receptor signaling, Toll-like receptor signaling, complement and coagulation cascades, and Th1 and Th2 cell differentiation pathway groups. These pathways were primarily related to the immune response of the host to virus infection (Fig.4-E). The DEPs annotated in the disease category are shown in Fig.4-F. There are ten pathways associated with infectious diseases, five of which are associated with viral infections.

According to the profiling of DEPs, a relatively large number of proteins matched with the MAPK signaling pathway, including FGF13, ERK5, and MKK3. The KEGG pathway analysis revealed that MKK3 is involved in 14 pathways, indicating that MKK3 is a key regulatory protein during BPIV3 infection of MDBK cells (Fig. 4-C).

Validation of the selected proteins by real-time quantitative PCR (qRT-PCR)

To verify the DEPs identified by iTRAQ, the transcriptional levels of eight proteins were measured by qRT-PCR. In this study, eight proteins were randomly selected for qRT-PCR. The

four upregulated proteins included AP-2 complex subunit beta protein (AP-2), FGF13, myristoylated alanine-rich C-kinase substrate (MARCS), and MKK3 proteins. The four downregulated proteins included MHC class II (MHCII), glutathione S-transferase (GSTA1), selenium protein P (SepP), and tissue factor pathway inhibitor (TFPI). As shown in Fig.5, the expression levels of these genes were consistent with the iTRAQ results. The results of qRT-PCR further verified the reliability of the iTRAQ experiment.

The effect of the p38 MAPK pathway on BPIV3 replication

BPIV3 infection activates the p38 MAPK pathway

The MAPK pathway plays various roles in intracellular signaling network. MKK3 and MKK6 are recognized as upstream kinases of p38. The results of proteomics analysis showed that the MKK3 level was significantly upregulated after BPIV3 infection (Fig. 4C). Virus infection is considered as an extracellular stimulant that can activate p38 MAPK pathway[18, 19]. It should be investigated whether BPIV3 infection activated the p38 MAPK pathway after MKK3 activation.

The expression of MKK3, p38, and phospho-p38 in BPIV3-infected cells was detected by western blotting assay. Cell samples were collected at 6, 12, and 24 h after BPIV3 infection. Compared to the mock group, the MKK3 expression levels were increased at different infection time points in the infected group. No change was observed in the p38 protein expression level, while the phospho-p38 expression level was significantly higher in the infected group than in the mock group at 12 and 24 h after BPIV3 infection (Fig. 6). Thus, BPIV3 infection induced MKK3 activation and p38 phosphorylation. The MKK3 expression level was consistent with previous proteomics results, which further verified the reliability of proteomics analysis.

The effect of inhibiting p38 MAPK activation on BPIV3 replication

To investigate whether the activation of the p38 MAPK pathway promotes BPIV3 proliferation, the cells were treated with SB202190, an inhibitor of the p38 MAPK pathway, 1 h before infection. MDBK cells were treated with SB202190 at 1.25, 5, and 10 M concentrations. Cell samples were collected at 24 h after infection (MOI = 1).

The results are shown in Fig. 7. BPIV3 infection induced the phosphorylation of p38. After treatment with the inhibitor SB202190, the expression level of p38 was significantly decreased in a dose-dependent manner, indicating that the phosphorylation of p38 was inhibited by SB202190(Fig.7-A). The results are shown in Fig. 7B. The BPIV3 virus titer decreased by 1.8 log$TCID_{50}$/mL after treatment with 10 M SB202190, indicating that the p38 MAPK pathway participates in the replication of BPIV3. The results showed that SB202190 could inhibit the proliferation of BPIV3. Thus, BPIV3 activated the p38 MAPK signaling pathway that is involved in its replication.

Discussion

iTRAQ LC-MS/MS is a powerful analytical tool for quantitative proteomics analysis that has been widely used in many studies [20-23]. Gray et.al used 2D gel electrophoresis proteomic to investigate in vitro cellular responses during BPIV3 infection [24]. In the present study, we first applied the iTRAQ LC-MS/MS approach to determine the profiles of DEPs in MDBK cells infected with BPIV3 at various time points of infection. A total of 116 DEPs were identified at 24 h after infection based on a fold change of ≥ 1.5 and p-value < 0.05 (data not show). On the basis of GO analysis, the DEPs were classified into 19, 11, and 9 categories for biological processes, cellular components, and molecular functions, respectively (Fig. 3). The pathway analysis identified the pathways based on the number of DEPs (Fig. 4). These data could provide a basis for understanding the pathogenetic mechanisms of BPIV3 infection.

The results showed that the PI3K-Akt signaling pathway and the MAPK signaling pathway play important roles in the progression of BPIV3 infection. According to the profiles of DEPs in these two signaling pathways, only ITGB3 was downregulated, while the remaining proteins were upregulated. The analysis of the DEPs in these pathways showed that the number of matched proteins in the MAPK signaling pathway was relatively large, including FGF13, ERK5, and MKK3. The KEGG pathway results indicated that MKK3 was involved in 14 pathways, which suggested that MKK3 is a key regulatory protein during BPIV3 infection. Previous studies have shown that the MAPK signaling pathway is a target of respiratory viruses, which regulates various stages of the infection process[25, 26].

The MAPK cascade plays various roles in intracellular signaling network pathways. MKK3 and MKK6 are recognized as upstream kinases of p38 that can directly phosphorylate tyrosine and serine/threonine residues to activate p38 [27]. Viral infection is thought to be an extracellular stimulant that activates this pathway. In infectious salmon anemia virus (ISAV) infection, immunohistochemical detection showed that the phosphorylation level of p-ERk1/p-p38 in the lungs of sheep infected with JSRV was significantly increased compared to that in healthy sheep [18]. In HBV-infected HuH-7 cells, the results showed that HBV replication activated JNK and p38 [30]. In our proteomics study, the MKK3 level was significantly upregulated 24 h after BPIV3 infection as compared to that in the control group. Therefore, we detected the expression level of the p38 MAPK pathway proteins after BPIV3 infection.

First, we investigated whether BPIV3 infection activates the p38 MAPK pathway. The results showed that BPIV3 induces the phosphorylation of p38 after infection. Compared to the control group, the phosphorylated p38 expression was significantly increased after 6 h of BPIV3 infection, demonstrating that BPIV3 can induce the activation of the p38 MAPK pathway in the early stage of infection.

Multiple extracellular stresses activate the MKK3-p38 MAPK cascade, including specific antigens, proinflammatory cytokines, ultraviolet light, heat shock, and other stress responses[28]. In accordance with the results of the mechanism of Coxsackie virus activation of p38 MAPK, we hypothesized that in the early stage of infection [29], the binding of BPIV3 HN protein to the

receptor on the surface of the cell membrane induced membrane fusion, and the cascade reaction of MKK3-p38 MAPK was temporarily activated. The progression of BPIV3 infection was gradually prolonged, and the phosphorylation of p38 MAPK was significantly increased 24 h after infection. In the late stage of infection, p38 was still continuously activated, which was speculated to be due to the release of proinflammatory cytokines induced by BPIV3 infection; the release of proinflammatory cytokines into the extracellular domain bound to the receptor further enhanced the activation of the p38 MAPK pathway[30, 31].

Many studies have shown that p38 is required for the replication of viruses. The activation of the MAPK pathways by viruses such as stimulates the JNK and p38 MAPK pathways to promote the release of virions[29]. In porcine reproductive and respiratory syndrome virus infection, the virus replication was inhibited after inhibition of the JNK and p38 pathways [32]. The same results were noted in PEDV infection[33]. To detect the role of the p38 MAPK pathway in BPIV3 replication, virus titer and CPE were analyzed. The results showed that the inhibitor SB202190 significantly inhibited virus replication in a dose-dependent manner. It was also found that p38 expression was inhibited after treatment with SB202190. Compared with the untreated group, virus titer was significantly decreased after treatment of the cells with the inhibitor. The inhibitor also showed a significant inhibitory effect on virus-induced CPE in a dose-dependent manner. These results revealed that the activation of the p38 MAPK pathway facilitated replication of BPIV3.

Conclusion

In this study, DEPs in BPIV3-infected MDBK cells were identified and quantitatively analyzed by iTRAQ and LC-MS-based proteomics analysis. Most of the DEPs were proteins related to inflammatory response, immune response, and lipid metabolism. Although many significantly up- or downregulated proteins and pathways are closely related to the symptoms or pathological responses to BPIV3 infection, further functional investigations are required to understand the pathogenic mechanisms and molecular responses of host cells to BPIV3 infection.

The results of the present study indicated that BPIV3 infection activates the p38 MAPK pathway, which is essential for its replication. Proteomics and western blot analyses showed that BPIV3 infection activated the p38 MAPK signaling pathway. Our future research will focus on which step of virus replication is affected by p38 activation.

Abbreviations

BPIV3: Bovine parainfluenza virus type 3; BRDC: bovine respiratory disease complex; iTRAQ: isobaric tags for relative and absolute quantitation analysis; DEPs: differentially expressed proteins; TGEV: transmissible gastroenteritis virus; PEDV: porcine epidemic diarrhea virus; BRSV: bovine respiratory syncytial virus; DMEM:Dulbecco's modified Eagle's medium; FBS:fetal bovine serum; CPE:cytopathic effect; GO: Gene Ontology; IFA: indirect immuno-fluorescent assay; MOI:multiplicity of infection; IL-13:interleukin-13; MAPK7: mitogen-

activated protein kinase 7; Foxp3: FOX transcription inhibitory factor 3; MARCS: myristoylated alanine-rich C-kinase substrate; MHCII: MHC class II; GSTA1: glutathione S-transferase; SepP: selenium protein P; TFPI: tissue factor pathway inhibitor.

Declarations

Acknowledgments

Not applicable.

Funding

This project was supported by the Heilongjiang Bayi Agricultural University natural science talent project (ZRCQC201808), Heilongjiang Agricultural Administration Bureau scientific research projects (HKKYZD190305), Post-doctoral Scientific Foundation of HeiLongJiang Province (LBH-Z20204), Heilongjiang Bayi Agricultural University Doctor's Research Foundation, (XDB201816), Heilongjiang Bayi Agricultural University Scientific Research Team Support project (TDJH201904).

Authors' contributions

All authors revised the manuscript.

Availability of data and material

Not applicable.

Ethics approval and consent to participate

Not applicable.

Consent to publication

Not applicable.

Competing interests

The authors declare that there are no conficts of interest.

Author details

a College of Life Science and Biotechnology, Heilongjiang Bayi Agricultural University, Daqing 163319, China. b College of Animal Science and Veterinary Medicine, Heilongjiang Bayi Agricultural University, Daqing 163319, China . c Department of Nephrology, The Fifth Affiliated Hospital of Harbin Medical University, Daqing 163319, China

References

1. Kale M, Dylek O, Sybel H, et al. Some viral and bacterial respiratory tract infections of dairy cattle during the summer season. Acta Vet-Beogr 2013, 63(2-3):227-236.
2. Kirchhoff J, Uhlenbruck S, Goris K, et al. Three viruses of the bovine respiratory disease complex apply different strategies to initiate infection. Vet Res 2014, 45:12.
3. Grissett GP, White BJ, Larson RL. Structured Literature Review of Responses of Cattle to Viral

and Bacterial Pathogens Causing Bovine Respiratory Disease Complex. J Vet Intern Med 2015, 29(3):770-780.

4. Ellis JA. Bovine Parainfluenza-3 Virus. Vet Clin N Am-Food Anim Pract 2010, 26(3):575-+.
5. Durbin AP, McAuliffe JM, Collins PL, et al. Mutations in the C, D, and V open reading frames of human parainfluenza virus type 3 attenuate replication in rodents and primates. Virology 1999, 261(2):319-330.
6. Bousse T, Takimoto T. Mutation at residue 523 creates a second receptor binding site on human parainfluenza virus type 1 hemagglutinin-neuraminidase protein. Journal of Virology 2006, 80(18):9009-9016.
7. Jardetzky TS, Lamb RA. Activation of paramyxovirus membrane fusion and virus entry. Curr Opin Virol 2014, 5:24-33.
8. Gerold G, Bruening J, Pietschmann T. Decoding protein networks during virus entry by quantitative proteomics. Virus Res 2016, 218:25-39.
9. Seggerson K, Tang LJ, Moss EG. Two genetic circuits repress the Caenorhabditis elegans heterochronic gene lin-28 after translation initiation. Dev Biol 2002, 243(2):215-225.
10. An K, Fang LR, Luo R, et al. Quantitative Proteomic Analysis Reveals That Transmissible Gastroenteritis Virus Activates the JAK-STAT1 Signaling Pathway. J Proteome Res 2014, 13(12):5376-5390.
11. Sun DB, Shi HY, Guo DH, et al. Analysis of protein expression changes of the Vero E6 cells infected with classic PEDV strain CV777 by using quantitative proteomic technique. J Virol Methods 2015, 218:27-39.
12. Li LY, Yu LY, Hou XL. Cholesterol-rich lipid rafts play a critical role in bovine parainfluenza virus type 3 (BPIV3) infection. Res Vet Sci 2017, 114:341-347.
13. Zhu YM, Shi HF, Gao YR, et al. Isolation and genetic characterization of bovine parainfluenza virus type 3 from cattle in China. Vet Microbiol 2011, 149(3-4):446-451.
14. Chowdhury SI, Coats J, Neis RA, et al. A bovine herpesvirus type 1 mutant virus with truncated glycoprotein E cytoplasmic tail has defective anterograde neuronal transport in rabbit dorsal root ganglia primary neuronal cultures in a microfluidic chamber system. J Neurovirol 2010, 16(6):457-465.
15. Yazici Z, Ozan E, Tamer C, et al. Circulation of Indigenous Bovine Respiratory Syncytial Virus Strains in Turkish Cattle: The First Isolation and Molecular Characterization. Animals 2020, 10(9):10.
16. Guo XZ, Hu H, Chen FZ, et al. iTRAQ-based comparative proteomic analysis of Vero cells infected with virulent and CV777 vaccine strain-like strains of porcine epidemic diarrhea virus. J Proteomics 2016, 130:65-75.
17. Khattri R, Cox T, Yasayko SA, et al. An essential role for Scurfin in CD4(+)CD25(+)T regulatory cells. J Immunol 2017, 198(3):993-998.
18. Olavarria VH, Recabarren P, Fredericksen F, et al. ISAV infection promotes apoptosis of SHK-1 cells through a ROS/p38 MAPK/Bad signaling pathway. Mol Immunol 2015, 64(1):1-8.
19. Fu YL, Yip A, Seah PG, et al. Modulation of inflammation and pathology during dengue virus infection by p38 MAPK inhibitor SB203580. Antiviral Res 2014, 110:151-157.
20. Li XF, Wang Q, Gao YN, et al. Quantitative iTRAQ LC-MS/MS Proteomics Reveals the Proteome Profiles of DF-1 Cells after Infection with Subgroup J Avian Leukosis Virus. Biomed Res Int 2015, 2015:10.

21. Lu Q, Bai J, Zhang LL, et al. Two-Dimensional Liquid Chromatography-Tandem Mass Spectrometry Coupled with Isobaric Tags for Relative and Absolute Quantification (iTRAQ) Labeling Approach Revealed First Proteome Profiles of Pulmonary Alveolar Macrophages Infected with Porcine Reproductive and Respiratory Syndrome Virus. J Proteome Res 2012, 11(5):2890-2903.
22. Hu F, Li YF, Yu KX, et al. Proteome analysis of reticuloendotheliosis-virus-infected chicken embryo fibroblast cells through iTRAQ-based quantitative proteomics. Arch Virol 2019, 164(12):2995-3006.
23. Zhong CY, Li JZ, Mao L, et al: Proteomics analysis reveals heat shock proteins involved in caprine parainfluenza virus type 3 infection. BMC Vet Res 2019, 15:14.
24. Gray DW, Welsh MD, Doherty S, et al. Identification of candidate protein markers of Bovine Parainfluenza Virus Type 3 infection using an in vitro model. Vet Microbiol 2017, 203:257-266.
25. Wang C, Wei D, Xu M, et al. The Role of p38MAPK in Acute Lung Injury Induced by H9N2 Influenza Virus Isolated from Swine. Acta Veterinaria et Zootechnica Sinica 2014, 45(2):281-288.
26. Lee N, Wong CK, Chan PKS, Lun SWM, et al. Hypercytokinemia and hyperactivation of phospho-p38 mitogen-activated protein kinase in severe human influenza a virus infection. Clin Infect Dis 2007, 45(6):723-731.
27. Coskun M, Olsen J, Seidelin JB, Nielsen OH. MAP kinases in inflammatory bowel disease. Clin Chim Acta 2011, 412(7-8):513-520.
28. Gautier A, Deiters A, Chin JW. Light-Activated Kinases Enable Temporal Dissection of Signaling Networks in Living Cells. J Am Chem Soc 2011, 133(7):2124-2127.
29. Si XN, Luo HL, Morgan A, Zhang JC, et al. Stress-activated protein kinases are involved in coxsackievirus B3 viral progeny release. Journal of Virology 2005, 79(22):13875-13881.
30. Pettus LH, Wurz RP. Small Molecule p38 MAP Kinase Inhibitors for the Treatment of Inflammatory Diseases: Novel Structures and Developments During 2006-2008. Current Topics in Medicinal Chemistry 2008, 8(16):1452-1467.
31. Choi MS, Heo J, Yi CM, Ban J, et al. A novel p38 mitogen activated protein kinase (MAPK) specific inhibitor suppresses respiratory syncytial virus and influenza A virus replication by inhibiting virus-induced p38 MAPK activation. Biochem Biophys Res Commun 2016, 477(3):311-316.
32. An TQ, Li JN, Su CM, Yoo D. Molecular and Cellular Mechanisms for PRRSV Pathogenesis and Host Response to Infection. Virus Res 2020, 286:11.
33. Lee C, Kim Y, Jeon JH. JNK and p38 mitogen-activated protein kinase pathways contribute to porcine epidemic diarrhea virus infection. Virus Res 2016, 222:1-12.

Figures

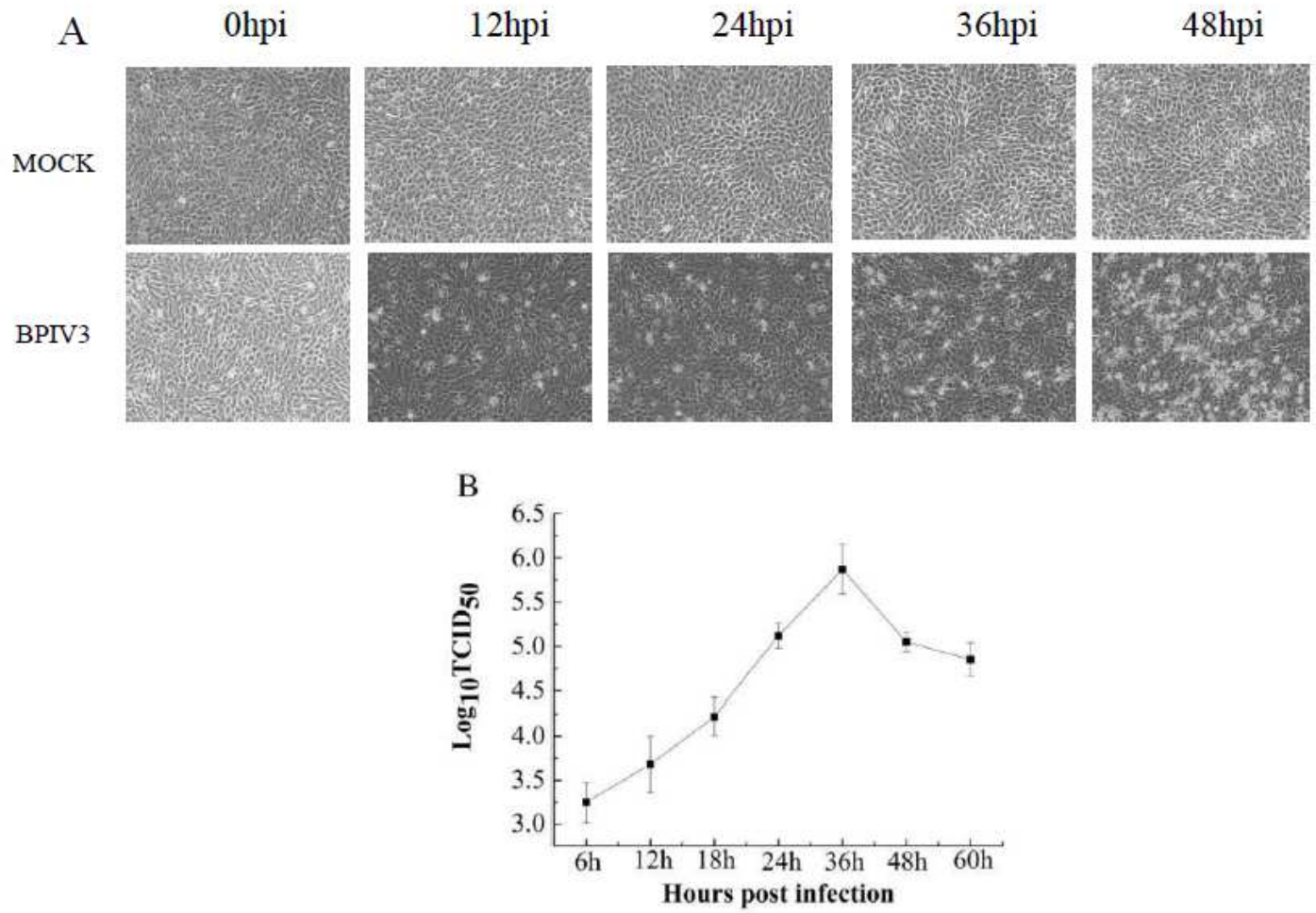

Figure 1

Virus infection. (A) Photomicrographs of MDBK cells infected with BPIV3 strain DQ at MOI = 1 or mock-infected at different times after infection (indicated at top). Images were taken at an original magnifification of 40×. (B) One-step growth curve of BPIV3 strain DQ in MDBK cells.

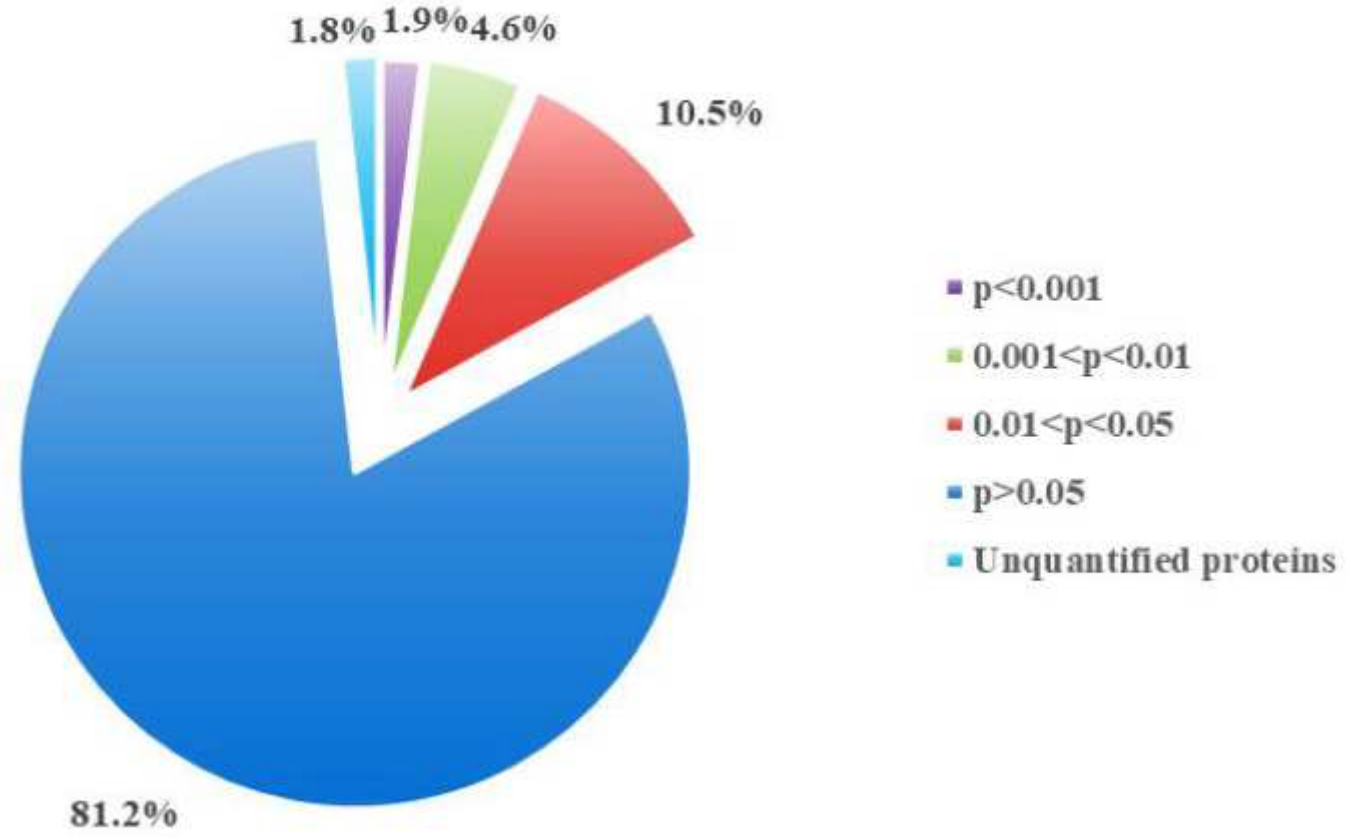

Figure 2

The quantitation and significance of the 2804 identified proteins from BPIV3-infected and mock-infected groups.

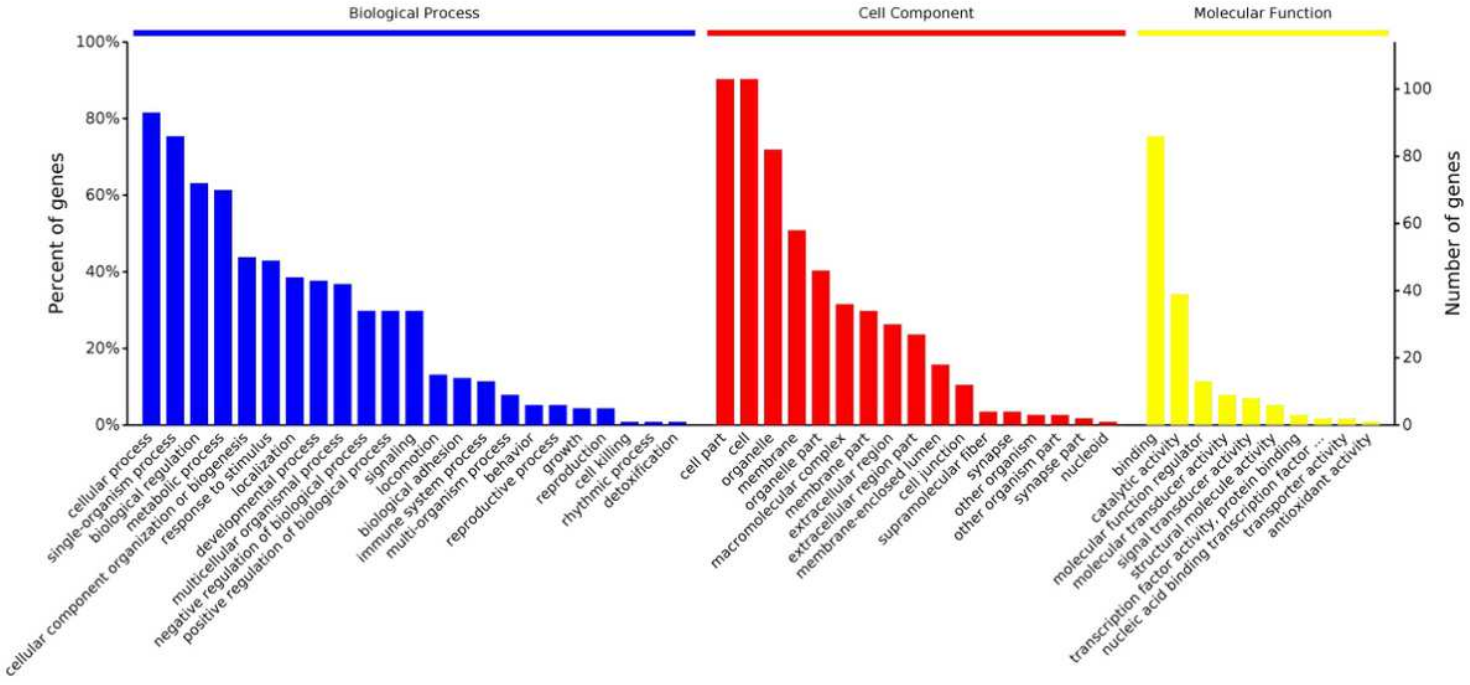

Figure 3

Gene ontology (biological process) analysis of the DEPs in BPIV3 groups vs. the control groups. The right coordinate axis indicates the number of proteins for each GO annotation, the down coordinate axis indicates the GO annotations. Blue stripes indicates that biological processes categories of DEPs; red stripes indicates that categories of cell components; yellow stripes indicates that categories of the molecular functions.

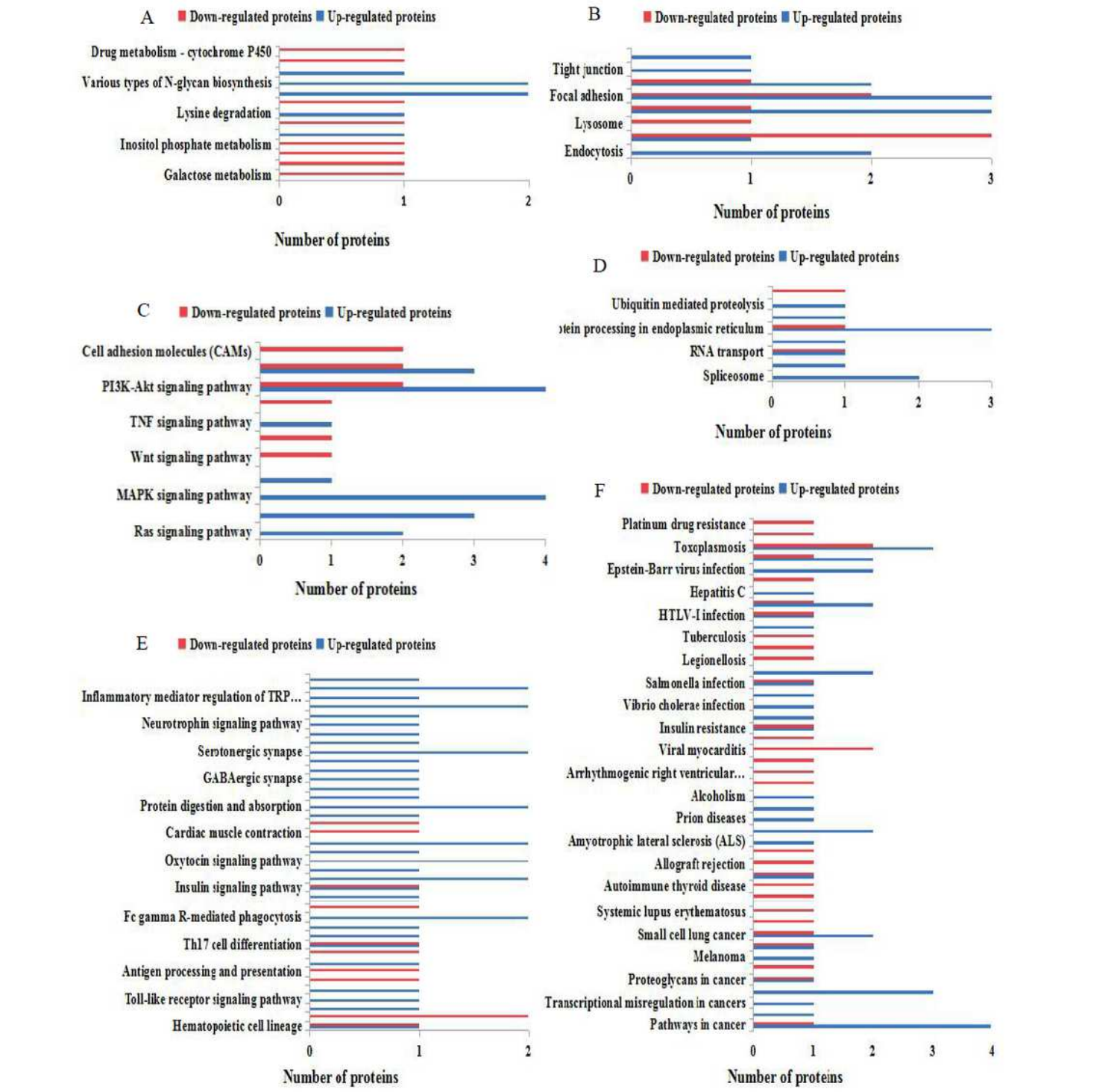

Figure 4

Analysis of the KEGG pathway of the differentially expressed proteins. (A) genetic information processing (B) Metabolism; (C) environmental information processing; (D) cellular processes; (E) organismal systems; (F) diseases.

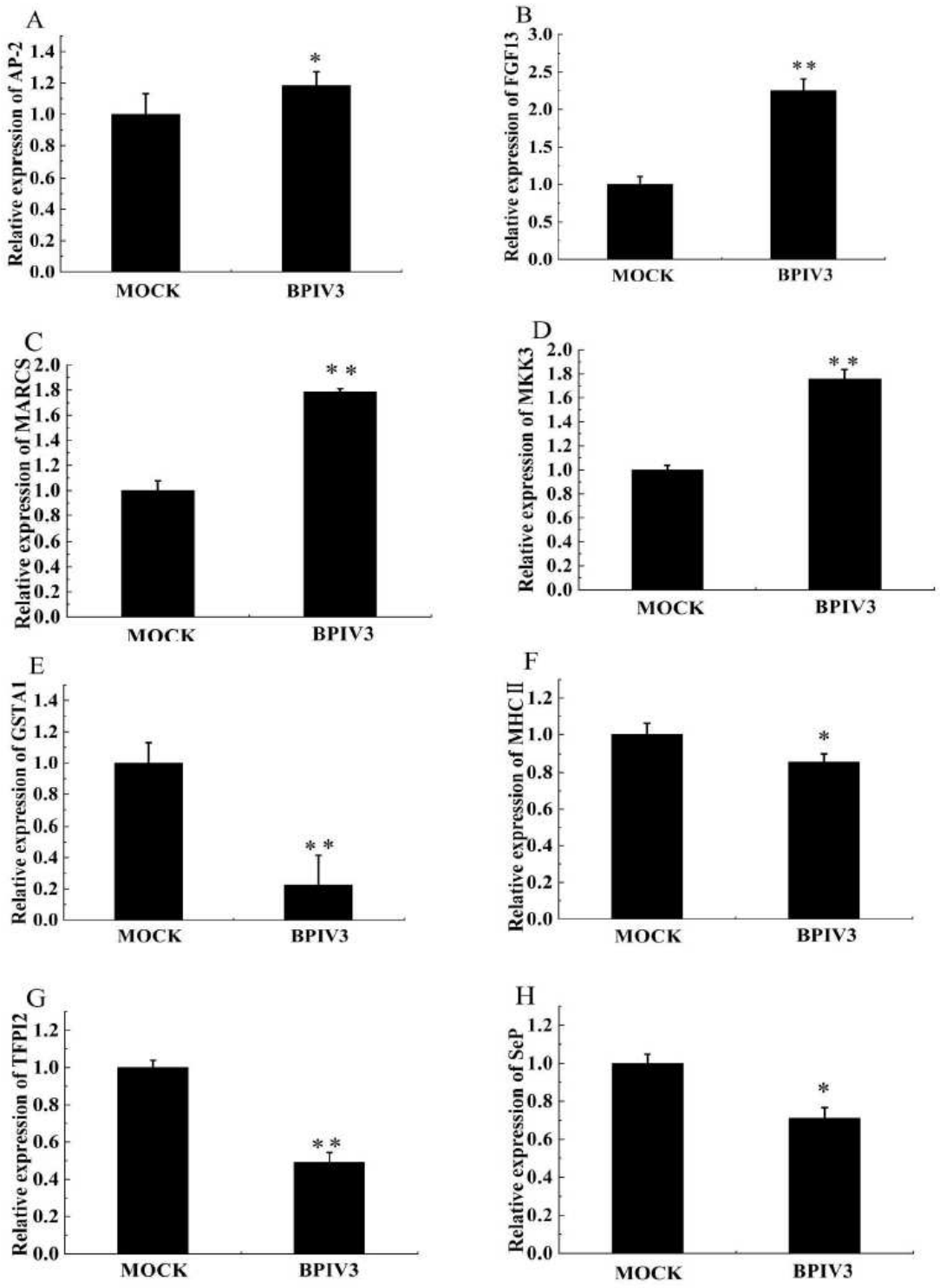

Figure 5

Real-time RT-PCR analysis of the DEPs in BPIV3-infected cells and controls. MDBK cells were infected with BPIV3 at MOI=1or mock-infected. The cells were collected at 24 hpi for real-time RT-PCR to analyze

the relative expression of 8 differential expression genes. (A).Relative expression of AP-2; (B) Relative expression of FGF13; (C) Relative expression of MARCS; (D) Relative expression of MKK3; (E) Relative expression of GSTA1; (F) Relative expression of MHCII; (G) Relative expression of TFPI2; (H) Relative expression of SepP.

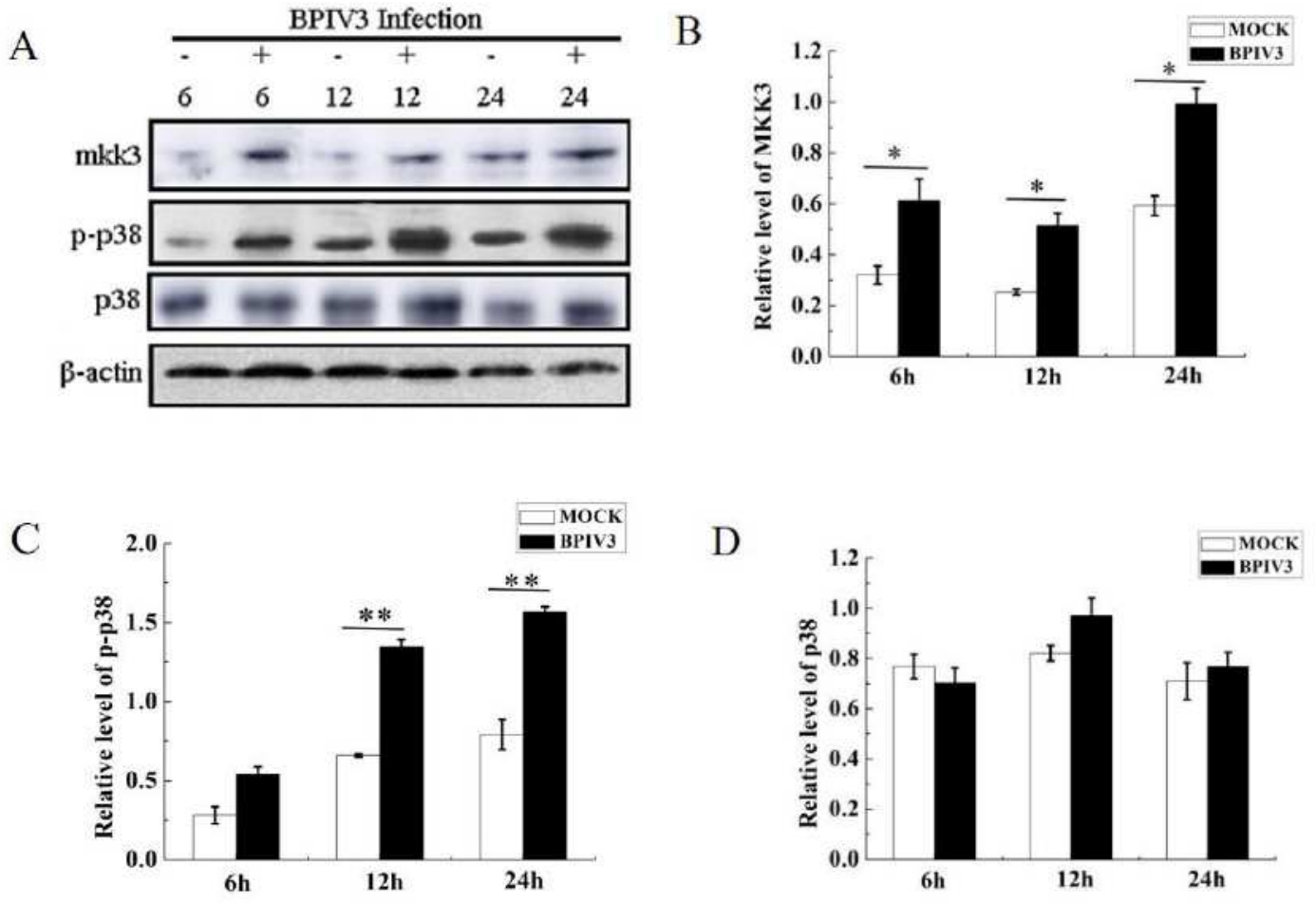

Figure 6

P38 MAPK pathway was activated by BPIV3 infection. (A) MDBK cells were mock-infected or infected with BPIV3 at multiplicity of infection (MOI) of 1 from 6 to 24 h, MKK3, p38 phosphorylation and total amount of p38 were analyzed in whole-cell lysates by Western blot with a specific mouse anti-phospho-p38 (9216, CST, USA), rabbit anti-p38 (41666, CST, USA) and rabbit anti-MKK3 (5674, CST, USA) antibodies followed by second antibody. β-actin probed with specific monoclonal antibody was served as loading control. Densitometry scans were conducted using ImageJ software (NIH, USA). Densitometry of the phospho-p38 band normalized to p38 is presented as fold change ± SEM compared with the mock-infected control defined as 1. These data were from three independent experiments. Significant differences compared with mock-infected control are denoted by *($P < 0.05$), ** ($P < 0.01$). The Same densitometry analysis and statistical analysis were performed in the following experiments. (A) The protein expression in p38 MAPK pathway by Western blot; (B) Expression of MKK3; (C) Expression of p-p38; (D) Expression of p38

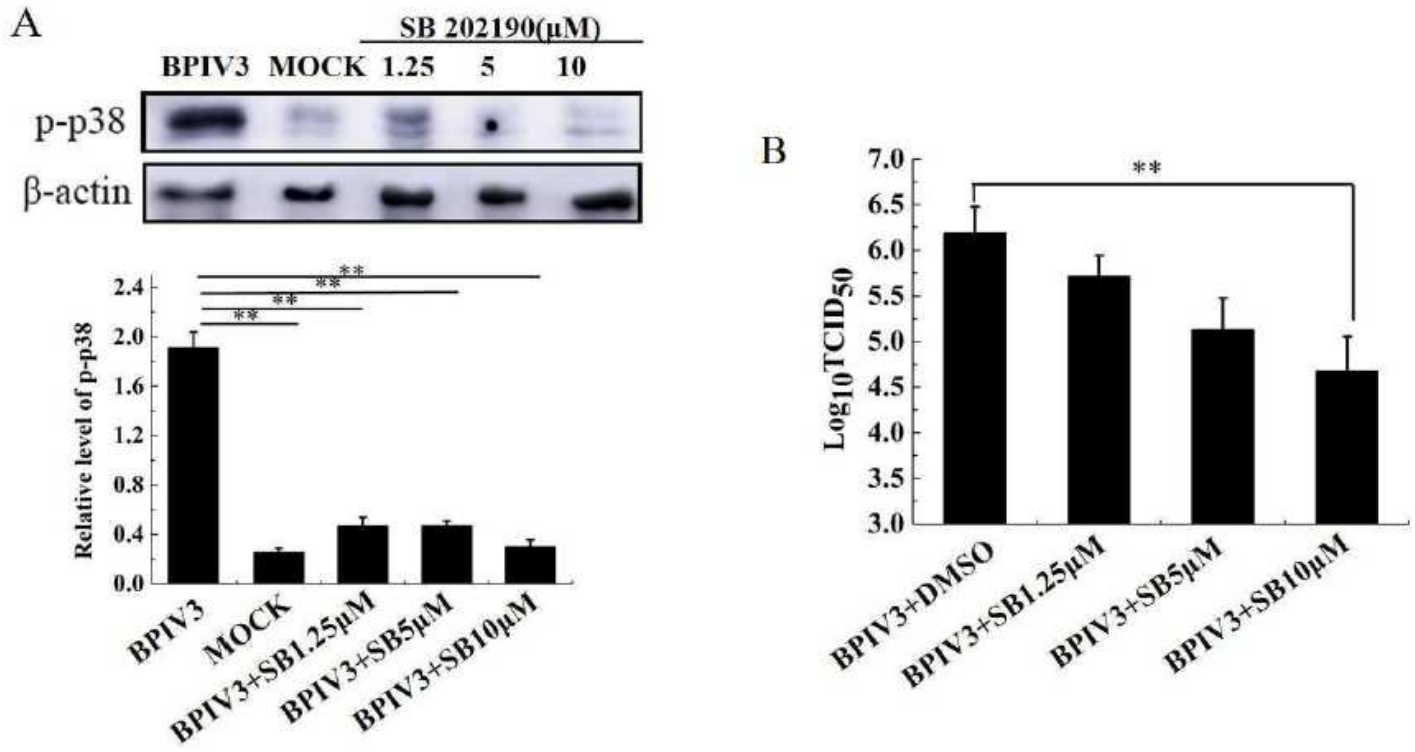

Figure 7

Inhibition of activation of the p38 pathway inhibits BPIV3 replication. MDBK cells were treated with SB202190 at 1.25, 5, and 10 M concentrations. After 1 h, BPIV3-infected cells were inoculated with MOI=1. Cell samples were collected at 24 h after infection, and the following tests were performed: (1) Cell samples were collected 24 h after infection, lysed with cell lysate, and the expression of phospho-p38 and β-actin in the samples was detected by Western-blot. (A) SB202190 impact on p38MAPK phosphorylation; (B) The cell supernatant was collected 24 h after infection, and the titer of the virus was detected by TCID50 assay.SB202190 impact on Bpiv3 TCID50.** ($P < 0.01$)